Desalination and Water Treatment
www.deswater.com
doi: 10.5004/dwt.2021.27778

238 (2021) 207–217
October

Effective removal of heavy metals from water by apatitic tricalcium phosphate subjected to different thermal treatments

Sonia Jebri[a,*], José Maria da Fonte Ferreira[b], Ismail Khattech[c]

[a]*Laboratory of Desalination and Valorization of Natural Water, Water Researches and Technologies Center, Technologic Park of BorjCedria, B.P. 273, Soliman 8020, Tunisia, email: sonia.jebri@gmail.com*
[b]*Department of Materials and Ceramics Engineering, CICECO-Aveiro Institute of Materials, University of Aveiro, 3810-193 Aveiro, Portugal, email: jmf@ua.pt*
[c]*Materials Cristal Chemistry and Applied Thermodynamics Laboratory, Chemistry Department, LR15SE01, Faculty of Science, Université de Tunis El Manar, Tunis 2092, Tunisia, email: ismail.khattech@fst.utm.tn*

Received 5 May 2021; Accepted 9 September 2021

ABSTRACT

In this study, tricalcium phosphate was prepared through a fast precipitation route at room temperature and then subjected to heat treatments within the temperature range of 100°C-900°C. Based on Fourier-transform infrared spectroscopy and X-ray diffraction studies, the powders heated below 600°C were assigned to apatitic tricalcium phosphate (TCPa) whereas the calcination at 900°C led to β-tricalcium phosphate (β-TCP) formation. The dried and calcined powders were tested as sorbents for cadmium in an aqueous medium. Their depolluting performance just slightly decreased with raising calcination temperature due to concomitant reductions in specific surface area (S_{BET}) and total volume of pores (V_p). Accordingly, the dried sample ($TCPa_{100}$) was selected to study the adsorption of relevant pollutant Cd^{2+} ions found in wastewaters. The adsorption capacity q_e was found to be 450 mg g^{-1} at 25°C, and increased to 493 mg g^{-1} by the rise in temperature to 45°C, indicating the endothermic nature of the adsorption process. In addition, the adsorption equilibrium was better described by the Freundlich model (R^2 = 0.9823), followed by Dubinin–Kaganer–Radushkevich (R^2 = 0.9739) and Langmuir model (R^2 = 0.9357). The morphological changes induced from this interaction were highlighted by scanning electron microscopy and transmission electron microscopy observations. Furthermore, the $TCPa_{100}$ removal efficiency of aqueous heavy metals such as lead (Pb^{2+}), copper (Cu^{2+}) and zinc (Zn^{2+}) from contaminated waters was evinced for single and multi-component pollution systems.

Keywords: Apatitic calcium phosphate; Heat treatment; Cadmium adsorption; Heavy metals

1. Introduction

Heavy metals are defined as comparatively-high density metallic elements that can cause toxicity even at low intaking doses [1,2]. Nowadays, water sources become more and more menaced by the continuous increase of urbanization, industrial activities, and the excessive use of chemicals all over the world [3]. The industrial contaminants commonly include ionic species of cadmium (Cd), lead (Pb), zinc (Zn) and copper (Cu). When released into the water systems above the permissible limits, these hazardous pollutants are of potential threat to the surrounding environment and to the aquatic organisms and public health. They can accumulate and be transferred up the food chain, threatening food safety and posing serious health risks [4]. Indeed, the bioaccumulation

* Corresponding author.

of these poisoning ions in human organisms leads to renal damage, osteoporosis and cancer diseases [5–7]. Therefore, continuous attempts have been made towards reducing these pollutants from contaminated sites. For this purpose, several remediation techniques have been developed such as chemical precipitation [8], membrane separation [9], ion exchange [10], and adsorption [11]. In spite of their availability to reduce different types of pollutants in wastewaters, the main drawbacks are related to economic and technological considerations. Interestingly, the adsorption method has the advantages of being highly efficient, economical, and simple to handle.

Among the large family of adsorbents, calcium phosphates such as hydroxyapatite $Ca_{10}(PO_4)_6(OH)_2$ (HAp) and tricalcium phosphate $Ca_3(PO_4)_2$ (TCP), showed high efficiency in removing toxic metals from water owing to their ability to accommodate various divalent cations in their crystalline lattices, partially replacing Ca^{2+} ions. Such replacements are facilitated especially when the ionic species have similar ionic radii as in the case of Cd^{2+} (0.97 Å) and Ca^{2+} (0.99 Å) [12]. Nevertheless, the ability of calcium phosphates to bound strange ionic species with significantly different ionic radii such as Sr^{2+} (1.20 Å), Ba^{2+} (1.35 Å), Pb^{2+} (1.19 Å), Cu^{2+} (0.73 Å) and Zn^{2+} (0.74 Å) and many other, including anions, has also been evinced in many published works [13–16].

Porosity and surface characteristics of HAp powders have been reported to be directly linked to the synthesis and heat treatment conditions due to the changes induced in the morphology or crystalline state of the starting powders, and that these features are likely to affect the reactivity of the sorbent materials with Cd^{2+} ions [17]. Heating the apatitic tricalcium phosphate (TCPa) at different temperatures is accompanied by important structural changes rather than simple textural modifications in which the Ca-deficient apatite takes different forms before its transformation to β-tricalcium phosphate [18]. In this way, the present study aims to investigate the effect of the calcination temperature of TCPa on its capacity for removing a series of heavy metal ions from contaminated water and to find out the most appropriate heat treatment conditions that allow maximizing the removal efficiency.

Among various heavy metals, cadmium was selected to study the adsorption possess since it is the contaminant most frequently found is wastewater. The main operating conditions were then applied to treat Pb^{2+}, Zn^{2+} and Cu^{2+} in single and multi-component systems.

2. Experimental

2.1. Chemical reagents

Calcium nitrate $Ca(NO_3)_2{\cdot}4H_2O$ (Sigma-Aldrich, United Kingdom) and diammonium phosphate $(NH_4)_2HPO_4$ (Fluka, USA) were used as precursors to synthesize the starting TCPa powder. Ammonia solution (28 wt.%) (Sigma-Aldrich, United Kingdom) was used for pH adjustments. The following reagents $Cd(NO_3)_2{\cdot}4H_2O$ (Sigma-Aldrich, United Kingdom), $Pb(NO_3)_2$ (Fluka, USA), $CuSO_4{\cdot}5H_2O$ (Carlo Erba), and $ZnCl_2$ (Sigma-Aldrich, United Kingdom), were adopted as sources of the contaminating ions Cd^{2+}, Pb^{2+}, Cu^{2+} and Zn^{2+}, respectively. All chemicals are of analytical grade and they were used without any further purification.

2.2. Powder synthesis

The starting TCPa powder was synthesized through a fast precipitation process at room temperature. The method consisted of: (i) preparing separately the precursor salt solutions [Solution A: calcium nitrate $Ca(NO_3)_2{\cdot}4H_2O$ (47.6 mmol), dissolved in 138 mL of deionized water; Solution B: diammonium phosphate $(NH_4)_2HPO_4$ (31.8 mmol) dissolved in 325 mL of deionized water]; (ii) Setting the alkalinity of both starting solutions to 10 by adding the required amounts of ammonia solution (28 wt.%); (iii) quickly pouring the Solution A into the Solution B under vigorous stirring. The synthesis can be described by the following scheme:

$$9Ca(NO_3)_2 + 6(NH_4)_2HPO_4 + 6NH_4OH \rightarrow 3Ca_3(PO_4)_2 + 18NH_4NO_3 + 6H_2O$$

The precipitate formed was immediately separated from the mother liquor by vacuum filtration, and then dried for 12 h at 100°C. Finally, the as-obtained dried powder was subjected to further thermal treatments by holding for 12 h at different calcination temperatures within the 200°C–900°C range in a Nabertherm muffle furnace, using a heating rate of 20°C min^{-1}.

2.3. Characterization techniques

An array of different characterization techniques was used to assess the relevant features of the heat-treated powders. X-ray diffraction analysis (XRD) was carried out at room temperature using a D8 ADVANCE Bruker diffractometer (Germany) with copper radiations ($K\alpha_1$ = 1.5406 Å; $K\alpha_2$ = 1.5445 Å) produced at 40 mA and 40 kV. Data were collected within the 2θ range between from 10° to 80° with a 2θ-step size of 0.01947° 2θ/s. The reference intensity ratio (RIR) method was used to determine the (semi-) quantitative crystalline phase analysis of the powder samples.

The Fourier-transform infrared (FTIR) spectra were recorded on IRAffinity-1 Shimadzu spectrophotometer (USA) within the wavenumber range from 400 to 4,000 cm^{-1}. The measurements were conducted on pellets prepared by mixing 1.0 mg of the sample with 200 mg of KBr for spectroscopic purposes. The impact of calcination temperature on the textural properties of TCPa was studied by N_2 adsorption–desorption on the material surface. The isotherms were performed with a Micromeritics ASAP 2020 (Bruxelles) at 77 K. The S_{BET} of the particles was calculated using Brunauer-Emmett-Teller (BET) method in the range of relative pressure (p/p^0) from 0.01 to 0.99. Morphological observations of the adsorbent surfaces were performed using Ultra-High Resolution Analytical Electron Microscope HR-FESEM Hitachi SU-70 (Japan) and transmission electron microscope (Hitachi, H9000 NAR). The distribution of elements within the adsorbent surface was determined by X-ray fluorescence mapping (XFM). The changes in concentrations of heavy metals after interacting with the sorbent for 1 h were measured by means of atomic absorption spectrometer (AAS) type novAA® 350 Analytik Jena (Germany).

2.4. Removal of pollutant heavy metal ions from simulated wastewaters

Aqueous solutions of Cd^{2+}, Pb^{2+}, Cu^{2+} and Zn^{2+} ions with various concentrations were prepared by diluting stock solutions of $Cd(NO_3)_2{\cdot}4H_2O$, $Pb(NO_3)_2$, $CuSO_4{\cdot}5H_2O$ and $ZnCl_2$ at 1,000 mg L^{-1} of each M^{2+} ion concentration. The study of heavy metals sorption onto TCPa powders calcined at different temperatures was carried out through the batch equilibrium technique. The influence of the calcination temperature on the interaction between the adsorbent surface and divalent cations was firstly investigated for Cd^{2+} ions. The effects of the adsorbent amount, the initial metal concentration, the temperature of the solution as well as the coexistence of other heavy metals were also studied. The adsorption experiments were carried out by mixing 10–60 mg of adsorbent with 100 mL of Cd^{2+} solutions at various concentrations. To study the effect of pH variation, the acidity/alkalinity of the medium was varied from pH ~ 4 up to neutral conditions (pH ~ 7) by dropwise adding of 0.1 M aqueous solutions of HCl or NaOH. To ensure the establishment of the equilibrium extraction, the suspension was stirred for 1 h at 300 rpm and then sampled through a 0.45 μm syringe filter for further analysis of the remaining metal ions. The removal efficiency, R (%), of the metal ions onto TCPa and the equilibrium adsorption capacity, q_e (mg g^{-1}) were calculated using Eqs. (1) and (2), respectively:

$$R(\%) = \frac{C_0 - C_e}{C_0} \times 100 \tag{1}$$

$$q_e = (C_0 - C_e) \times \frac{V}{m} \tag{2}$$

where C_0 and C_e are the metal ion concentrations (mg L^{-1}) in the liquid phase, initially and after the equilibration time, respectively, V is the solution volume (L), and m is the used mass of TCPa powder (g). The equilibrium data were analyzed with Langmuir, Freundlich, and Dubinin–Kaganer–Radushkevich (DKR) isotherm models. Mathematically, these models are expressed by Eqs. (3)–(5), respectively:

$$\frac{C_e}{q_e} = \frac{1}{k_L q_m} + \left(\frac{1}{q_m}\right) C_e \tag{3}$$

$$\ln(q_e) = \ln(k_f) + \left(\frac{1}{n}\right) \ln(C_e) \tag{4}$$

$$\ln(C_{ads}) = \ln(q_s) - \beta\varepsilon^2 \tag{5}$$

In Eq. (3), q_m (mg g^{-1}) and k_L (L mg^{-1}) are the Langmuir isotherm parameters related to the sorption capacity and energy of adsorption, respectively. A constant separation factor (R_L) given by the relationship: $R_L = 1/(1 + k_L C_0)$ could be deduced from this model, giving important information about the adsorption process. Hence, R_L value indicates whether the adsorption process is irreversible ($R_L = 0$), linear ($R_L = 1$), favorable ($0 < R_L < 1$) or unfavorable ($R_L > 1$). In Eq. (4), k_f is the Freundlich isotherm constant, and n is an empirical parameter measuring the adsorption intensity, which varies with the adsorbent heterogeneity. Thus, if ($1/n$) values are in the range of 0.1 to 1, the adsorption conditions are favorable. In Eq. (5), C_{ads} (mol g^{-1}) is the number of metal ions adsorbed per unit mass of adsorbent and q_s (mol g^{-1}) is the theoretical saturation capacity, β (mol^2 J^{-2}) is an activity coefficient related to the mean free energy of adsorption per mole of the adsorbate, and ε (J mol^{-1}) is the Polanyi potential expressed as: $\varepsilon = RT \ln(1 + 1/C_e)$, where, R (J mol^{-1} K^{-1}) is the gas constant and T (K) is the absolute temperature of the equilibrium experiment. The determination of β constant gives an idea about the mean free energy, E (kJ mol^{-1}), which is expressed as: $E = (2\beta)^{-1}$. The extent of apparent energy E is useful to estimate the type of adsorption. Thereby, values of $E < 8$ kJ mol^{-1} indicate physical adsorption, whereas, for $8 < E < 16$ kJ mol^{-1}, the adsorption process is described by ion exchange, and over 16 kJ mol^{-1}, it is governed by stronger chemical adsorption rather than by ion exchange [19].

3. Results and discussion

3.1. Characterization of TCPa powders

3.1.1. FTIR spectroscopy

The FTIR spectra of the powders after drying (100°C) and further calcining within the temperature range of 200°C–900°C are displayed in Fig. 1. From now on, the resulting samples are generically labeled as $TCPa_T$ in which T stands for the calcination temperature.

The recorded spectra exhibit the characteristic absorbance bands of PO_4^{3-} groups located between 958–1,076 cm^{-1} and centered at 470, 561, and 600 cm^{-1}. Absorbance bands specific to OH^- groups of the apatite phase are also detected in the dried and in the further heated samples between 200°C–600°C. These bands, centered at 3,562 and 615 cm^{-1} are attributed to the stretching and vibrational modes, respectively, of OH^- ions. Moreover, an absorbance band assigned to HPO_4^{2-} groups is also detected, being centered at 860 cm^{-1}. It could be seen that the intensities of these bands tend to decrease with increasing the calcination temperature up to 600°C, disappearing from the spectrum of the calcined at 900°C. This disappearance suggests that the hill-defined and partially hydrated apatitic phase prevailing at lower heat treatment temperatures, has been transformed in the planned TCP phase at this temperature [18]. Furthermore, the progressive disappearance of the absorption band located at 1,383 cm^{-1}, attributed to nitrate groups [20] shows that the nitrate ions adsorbed onto the surface of the particles during the synthesis are gradually released and disappear for calcination temperatures above 400°C.

3.1.2. X-ray diffraction

The XRD patterns of the dried and calcined powders are displayed in Fig. 2. They confirm that a hill-defined apatitic material has been precipitated and that the crystallographic features remained almost unaltered up to 600°C (Fig. 2a). All the powder samples heat-treated up to 600°C were identified as lacunar apatite calcium phosphates with the following chemical formula $Ca_9\square(HPO_4)(PO_4)_5OH\square$.

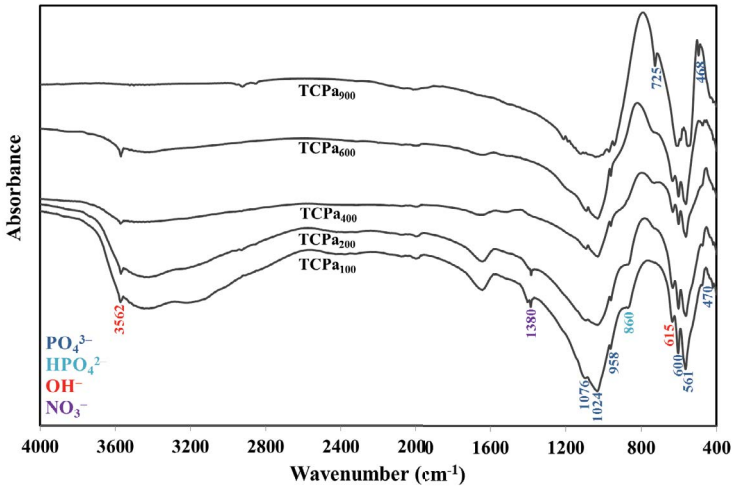

Fig. 1. FTIR spectra of TCPa powders calcined at different temperatures.

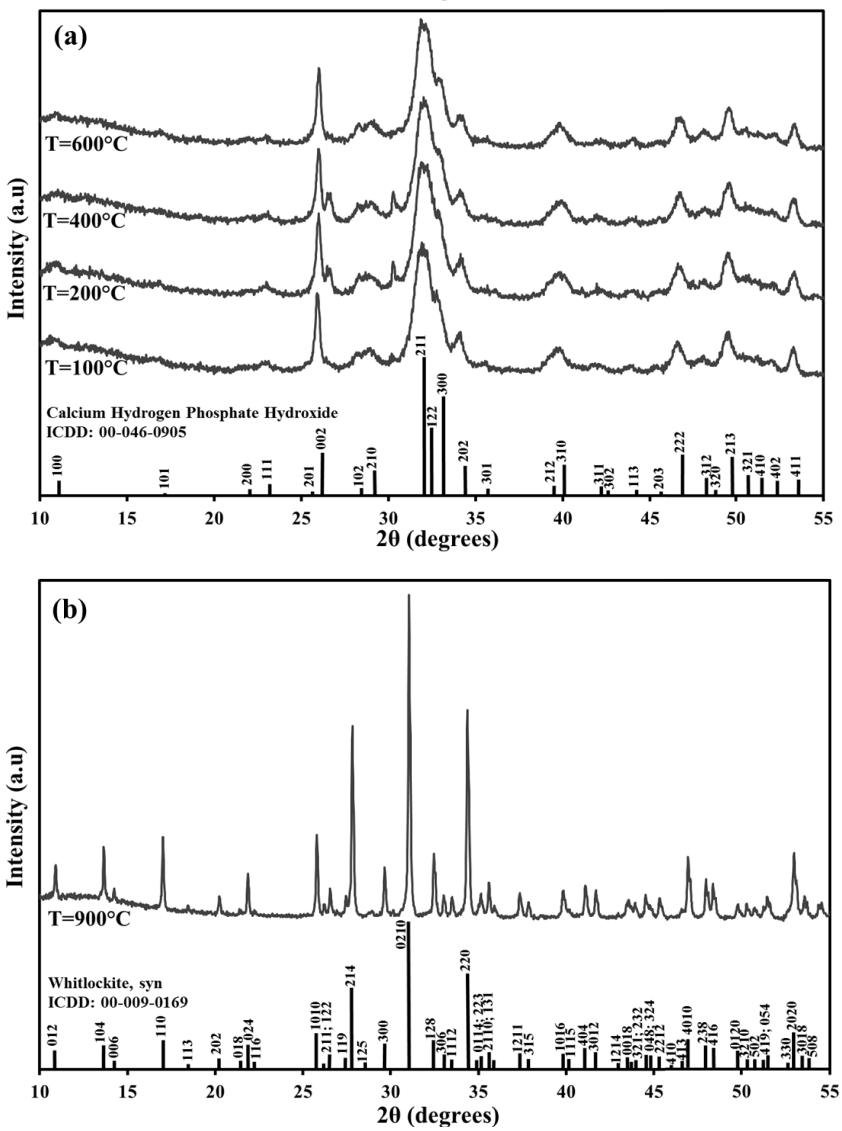

Fig. 2. X-ray diffraction patterns of TCP powders subjected to different thermal treatments: (a) from 100°C–600°C and (b) at 900°C.

The lattice parameters calculated for this phase using 'Eracel' software are: $a = b = 9.515 \pm 0.015$ Å and $c = 6.931 \pm 0.007$ Å. Upon further increasing the calcination temperature to 900°C, the apatite phase was completely converted to a highly crystallized β-tricalcium phosphate $Ca_3(PO_4)_3$ (whitlockite) (Fig. 2b) with the following lattice parameters: $a = b = 10.442 \pm 0.003$ Å and $c = 37.412 \pm 0.009$ Å.

The following ICDD card numbers, # 00-046-0905, for calcium hydrogen phosphate hydroxide ($Ca_9HPO_4(PO_4)_5OH$), and # 00-009-0169 for whitlockite, syn, were used to identify the crystalline phases. These results confirm that there is a good agreement between the observed XRD results and the data gathered by FTIR (Fig. 1).

3.1.3. Effects of the heat treatments on the textural properties

To highlight the effects of the heat treatments on the surface properties of the powders, the samples $TCPa_{100}$ and $TCPa_{900}$ were subjected to the physic-sorption of N_2. The resulting adsorption–desorption isotherms are depicted in Fig. 3. From these results, it can be concluded that the samples are predominantly mesoporous, as evidenced by their type IV isotherms. However, the dried material exhibits a higher hysteresis loop (at $p/p^0 > 0.8$) compared to that calcined at 900°C ($0.12 < p/p^0 < 0.70$). The data collected in Table 1 reveal that calcination at 900°C caused drastic decreases in the textural parameters, especially in the specific surface area (S_{BET}) (~24 times), and total pore volume (V_p) (127 times). The C_{BET} value measures the adsorption force of the first adsorbed nitrogen layer, being therefore directly related to the affinity of nitrogen toward the material surface [21]. The decrease of C_{BET} to less than one fifth indicates a much lower affinity of nitrogen toward the surface of the $TCPa_{900}$ sample.

3.2. Evaluation of the sorption performance of polluting heavy metal ions

3.2.1. Effects of the heat treatments

To study the impact of the heat treatments on the removal efficiency of aqueous cadmium ions, doses of 0.2 g L^{-1} of the powders were equilibrated with Cd^{2+} solutions at predefined temperatures for initial concentrations of 10 and 100 mg L^{-1}. This difference in the initial metal concentrations was selected in order to evaluate the ability of the adsorbent materials in remediating diluted and highly concentrated Cd-contaminated waters. The results from both experiments are displayed in Fig. 4. It can be seen that a total neutralization of cadmium was achieved irrespective of the calcination temperature for the initial metal concentration of 10 mg L^{-1}. But when the initial metal concentration was increased to 100 mg L^{-1}, the removal efficiency slightly decreased and remained at around 90% with only an almost imperceptible decreasing

Table 1
Textural features of the TCPa powders after drying and further heat treated at 900°C

Temperature (°C)	S_{BET} ($m^2\ g^{-1}$)	V_p ($cm^3\ g^{-1}$)	D_p (Å)	C_{BET}
$TCPa_{100}$	94	0.508	216	127
$TCPa_{900}$	4	0.004	96	23

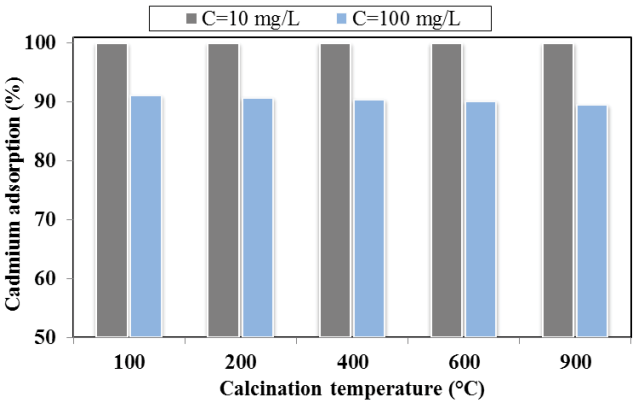

Fig. 4. Evolution of Cd^{2+} removal efficiency of TCPa powders heated treated at various temperatures. The adsorption experiments were conducted under the following conditions: $[Cd^{2+}]_0 = 10$ and 100 mg L^{-1}; adsorbent dosage = 0.2 g L^{-1}; temperature = 298 K; contact time = 1 h.

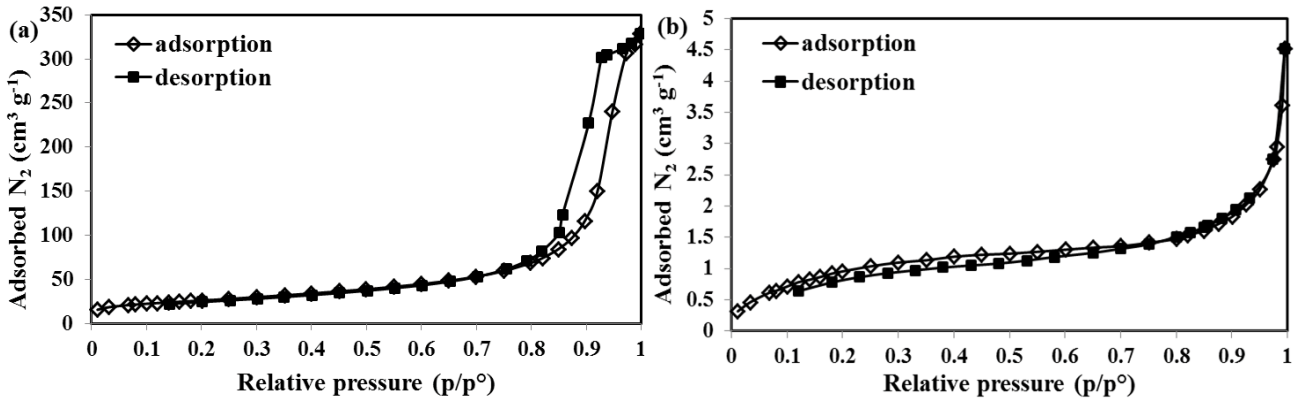

Fig. 3. Nitrogen adsorption–desorption isotherms for the samples: (a) $TCPa_{100}$ and (b) $TCPa_{900}$.

trend. Indeed, for a given amount of a specific absorbent, increasing the metal ion concentrations in the liquid phase tend to gradually saturate the active sites exposed onto the solid surface, therefore gradually reducing the driving force for the adsorption process to proceed further. Accordingly, higher metal ion concentrations (C_e values) will remain in the liquid phase after the equilibration time. In this way, the numerator of Eq. (1) decreases, explaining the observations made. This finding is somewhat surprising considering the significant reductions observed for the textural features of the material with the rise of calcination temperature. Moreover, it contrasts with the removal efficiency of Cd^{2+} ions by hydroxyapatite powders submitted to similar heat treatment schedules, as reported in our previous study where a significant dependence on calcination temperature was observed [17]. Thus, Cd^{2+} uptake in this case could be governed by stronger chemical adsorption rather than by physical sorption on the surface of the material. Based on these findings, the $TCPa_{100}$ sample was selected to study its ability to remove Cd^{2+} ions and other heavy metals that could exist in wastewaters.

3.2.2. Effect of the adsorbent dose

For evaluating the effect of the adsorbent dosage on Cd^{2+} uptake, different amounts of $TCPa_{100}$ were equilibrated with 10 mg L^{-1} of Cd^{2+} solution at 25°C. The results shown in Fig. 5 depict the variation of the removal percentage of the metal ions vs. adsorbent dosages varying within 0.1–0.6 g L^{-1}. It can be seen that a high percentage (87%) of the initial Cd^{2+} ions was neutralized by 0.1 g L^{-1} of adsorbent. Increasing the adsorbent dose to 0.2 g L^{-1} enhanced the removal percentage to 99.8%. The level of ~100% removal remained almost constant with further incremental amounts of sorbent. Accordingly, the optimum dosage of $TCPa_{100}$ for removing Cd^{2+} ions was found to be 0.2 g L^{-1} and thus, this amount was selected and used for further studies aiming at determining the maximum uptake capacity.

3.2.3. Effect of the initial Cd^{2+} concentration

In agreement with the findings in the previous section, the dosage of 0.2 g L^{-1} of $TCPa_{100}$ powder was used to evaluate the effect of the initial Cd^{2+} concentration on its removal percentage (%) at 25°C, as well as its uptake capacity (q_e). The $TCPa_{100}$ powder was equilibrated with Cd^{2+} solutions at initial concentrations varying within the range of 10–100 mg L^{-1}. The results displayed in Fig. 6 show a continuous and almost linear increase of q_e as a function of the initial Cd^{2+} concentration, meaning that the sorbent didn't undergo its saturation in sorbate. Furthermore, the removal percentage decreases with increasing metal ions concentration. In fact, at lower concentrations, the ratio of the initial number of metal ions to the available surface-active sites is low. At intermediate concentrations the fractional adsorption becomes independent of initial concentration, while at high concentrations the available sites for adsorption become fewer and, consequently, the removal percentage of metal becomes dependent upon the initial metal concentration.

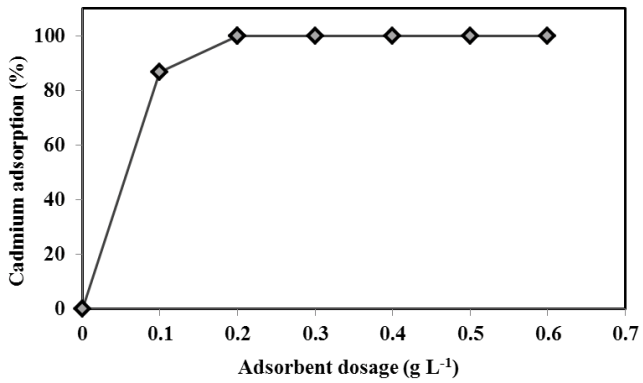

Fig. 5. Effect of sorbent dosage on Cd^{2+} removal efficiency of $TCPa_{100}$ (Conditions: $[Cd^{2+}]_0$ = 10 mg L^{-1}; pH = 5.2, contact time = 1 h; temperature = 298 K).

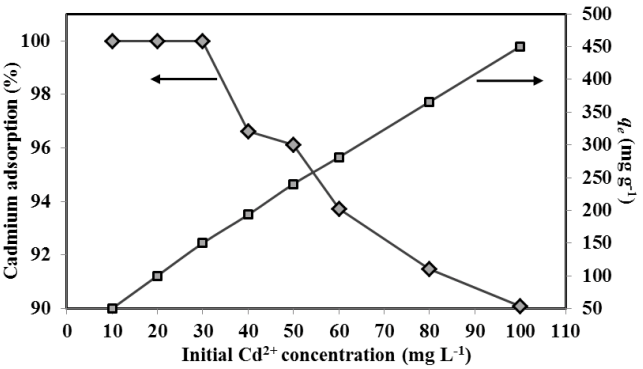

Fig. 6. Variation of the adsorption rate and the uptake capacity of Cd^{2+} onto $TCPa_{100}$ with initial metal concentration at 298 K (Conditions: adsorbent dose = 0.2 g L^{-1}; V = 100 mL; pH = 5.2; contact time = 1 h).

3.2.4. Effect of the temperature

The impact of the testing temperature on Cd^{2+} uptake by $TCPa_{100}$ has been studied at 303, 308, 313 and 318 K, for an initial metal concentration of 100 mg L^{-1}. The results displayed in Fig. 7 reveal that the adsorption capacity has gradually increased from ~455 to ~493 mg g^{-1} with the rise of the temperature, suggesting an endothermic nature of the adsorption process. This phenomenon was explained by an increase in the mobility of the metal ions that favors their interactions with the active surface sites. It was also reported that increasing temperatures may produce a swelling effect within the internal structure of the adsorbent, enabling large entities to cross the external boundary layer and reach the internal pores [22].

3.3. Adsorption isotherms and thermodynamic study

As stated in the experimental procedure, the ability of several adsorption isotherms models (Langmuir, Freundlich, and Dubinin–Kaganer–Radushkevich) for fitting the experimental adsorption equilibrium data was evaluated. These models were considered to be the most

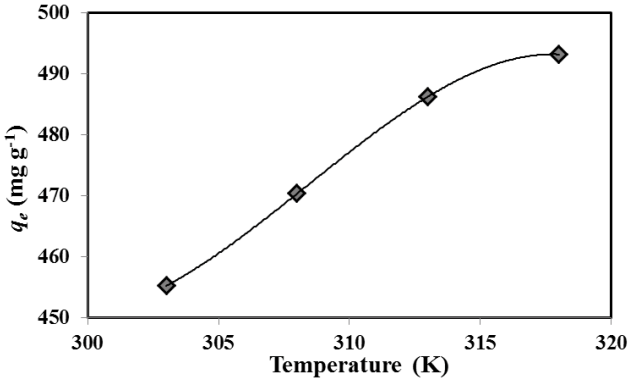

Fig. 7. Effect of the temperature on the uptake of Cd^{2+} ions by TCP_{100} (Conditions: $[Cd^{2+}]_0$ = 100 mg L^{-1}; V = 100 mL; adsorbent dose = 0.2 g L^{-1}; pH = 5.2; contact time = 1 h).

appropriate ones for equilibrium modelling of Cd(II) adsorption onto calcium phosphates [17,23]. Indeed, the parameters provided by these models give important information about the adsorption mechanisms and the type of interaction between adsorbent surface and adsorbed species. The basic assumptions of the Langmuir model include: (i) the formation of a monolayer onto the surface of the adsorbent with only one molecule of adsorbate being bonded on each adsorption site; (ii) the adsorbent surface is homogeneous in character, and the adsorption sites are identical and energetically equivalent. The Freundlich isotherm considers heterogeneous surfaces, while DKR model applies to adsorption processes occurring on homogeneous and heterogeneous surfaces.

Fig. 8a displays the experimental adsorption isotherm of Cd^{2+} on $TCPa_{100}$ at 25°C when the initial metal concentration was varied from 10 to 100 mg L^{-1}. The equilibrium data have been correlated with Langmuir (Fig. 8b) Freundlich (Fig. 8c) and DKR (Fig. 8d) models. A linear fit was obtained when C_e/q_e was plotted against C_e for the Langmuir isotherm. Similar trends were observed by plotting $\ln q_e$ vs. $\ln C_e$ and $\ln C_{ads}$ vs. ε^2 according to Freundlich and DKR modes, respectively. However, it could be seen that Freundlich isotherm is the one that best fits the experimental data (R^2 > 0.98). This confirms that adsorption occurs on a heterogeneous surface through a multilayer adsorption mechanism.

The parameters obtained from least-squares fits to the selected models, Eqs. (3)–(5), are gathered in Table 2. The maximum sorption capacity, q_m = 434.8 mg g^{-1}, was obtained for the Langmuir model. The R_L values are situated within the range of 0–1, indicating favorable adsorption of Cd^{2+} ions onto $TCPa_{100}$ under our experimental conditions. Furthermore, the $1/n$ factor determined from the Freundlich isotherm model is within the range of 0.1–1, also confirming favorable conditions for the occurrence of the adsorption process. The values of mean free energy, E, derived

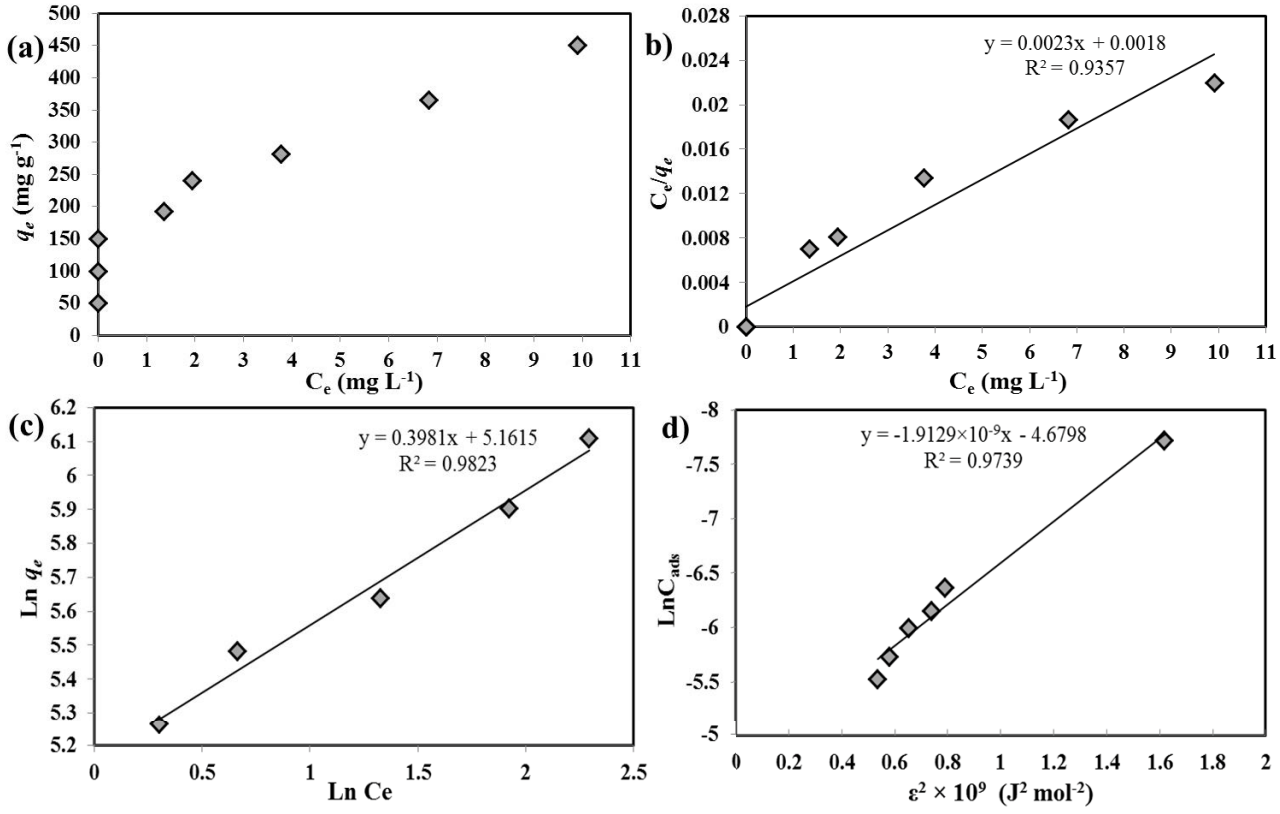

Fig. 8. (a) Isotherm of Cd^{2+} sorption onto $TCPa_{100}$, (b)–(d) linear fits of experimental data to the Langmuir, Freundlich and DKR models, respectively. (Conditions: temperature = 298 K; adsorbent dose = 0.2 g L^{-1}; initial pH = 5.2; contact time = 1 h).

Table 2
Isotherm parameters for the adsorption of Cd^{2+} onto $TCPa_{100}$ at 25°C

Isotherm model	Parameters	Values
Langmuir	q_m (mg g^{-1})	434.8
	k_L (L mg^{-1})	1.278
	R_L	0.072–0.008
	R^2	0.9357
Freundlich	k_f	174.4
	n	2.51
	R^2	0.9823
Dubinin–Kaganer–Radushkevich	q_s (mmol g^{-1})	9.28
	β (mol^2 J^{-2})	-1.91×10^{-9}
	E (kJ mol^{-1})	16.2
	R^2	0.9739

from the DKR model is 16.2 kJ mol^{-1}, suggest a chemisorption reaction involving the establishment of chemical bonds between the adsorbent's surface and the adsorbate. Finally, referring to R^2 values, it is clear that Freundlich isotherm shows the best fit for the adsorption of Cd^{2+} ions on $TCPa_{100}$ ($R^2 > 0.98$). This isotherm does not predict any saturation of the sorbate, and thus infinite surface coverage including multilayer adsorption is likely to occur.

Estimating the thermodynamic parameters such as Gibbs free energy (ΔG°), enthalpy (ΔH°) and entropy (ΔS°), is important to predict the prevailing type of adsorption process. These data could be determined through the changes of the equilibrium constant as a function of the testing temperature, based on the following Van't Hoff equation:

$$\ln K_d = -\frac{\Delta H^\circ}{RT} + \frac{\Delta S^\circ}{R} \quad (6)$$

where R is the universal gas constant (8.314 J mol^{-1} K^{-1}) and K_d is the distribution ratio of the metal between the solid and the liquid phase, expressed as: $K_d = q_e/C_e$.

Hence, ΔH° and ΔS° values are determined from the slope and intercept of the linear variation of lnK_d vs. 1/T as shown in Fig. 9. Whereas, ΔG° is deduced using the relationship: ΔG° = ΔH° – TΔS°. The calculated thermodynamic data are presented in in Table 3.

The positive value of ΔH° indicates an endothermic nature of the adsorption process. Furthermore, this quantity is higher than 40 kJ mol^{-1}, and consequently the interaction adsorbent–adsorbate is of chemical nature involving strong attractive forces. On the other hand, the positive value of ΔS° shows a rise in the disorder at the solid–liquid interface.

3.4. Morphological studies

The morphological features of the adsorbent before ($TCPa_{100}$) and after interaction with cadmium ($TCPa_{100}$-Cd) were determined by scanning electron microscopy observations. The results are shown in Fig. 10. The images indicate that the adsorption process induced significant morphological surface modifications. A clear enrichment of the solid

Table 3
Thermodynamic parameters for Cd^{2+} adsorption onto $TCPa_{100}$

ΔH° (kJ mol^{-1})	ΔS° (J mol^{-1} K^{-1})	ΔG° (kJ mol^{-1})			
		303 K	308 K	313 K	318 K
46.42	167	–4.19	–5.02	–5.86	–6.69

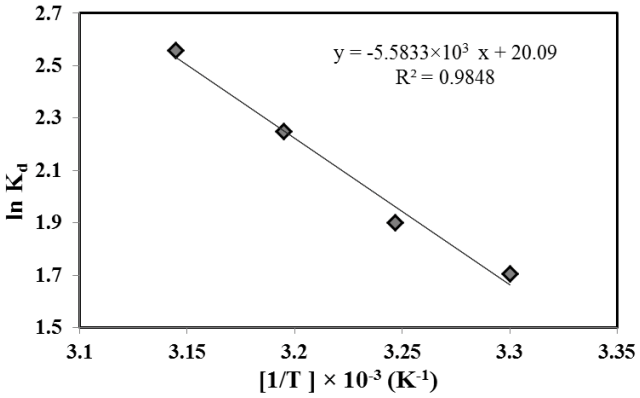

Fig. 9. Plot of lnK_d vs. 1/T for adsorption of Cd^{2+} onto $TCPa_{100}$.

in cadmium is well evidenced in the displayed energy-dispersive X-ray spectroscopy spectra. On the other hand, XFM associated to the transmission electron microscopy image shown in Fig. 11, reveal the distribution of calcium (Ca), cadmium (Cd) and phosphorus (P) within $TCPa_{100}$-Cd sample.

3.5. Interactions of sorbent with heavy metals

Considering that several heavy metals often coexist in wastewaters, the efficiency of the adsorption process in remediating aqueous heavy metals in single and multi-component pollution systems using $TCPa_{100}$ was investigated.

3.5.1. Single element systems

The sorption of single metal ions (Pb^{2+}, Cu^{2+}, Zn^{2+}) onto $TCPa_{100}$ powder was studied under the optimal conditions. The physical characteristics of the studied metals are summarized in Table 4 [24]. The experiments were conducted at 298 K with 100 mg L^{-1} of metal ion solutions, and the initial pH values were set to 4, 5, 6 and 7. The results plotted in Fig. 12 reveal that the adsorption of Pb^{2+} ions was not pH-dependent. However, pH plays an important role on Cd^{2+}, Cu^{2+} and Zn^{2+} immobilization by $TCPa_{100}$. Indeed, apatitic tricalcium phosphate synthesized under similar conditions was reported to exhibit a point of zero charge (PZC) at pH 5.6 [25]. Therefore, for pH values > 5.6, attractive electrostatic interactions between the negatively charged surface of $TCPa_{100}$ and the metal cations will foster the adsorption capacity. Whereas, acidification enhances the adsorption of H_3O^+ protons, conferring to the particles a positive surface charge, or a partial dissolution, which decrease the driving force for adsorbing metal cations at pH values < 5.6. No adsorption tests were conducted below

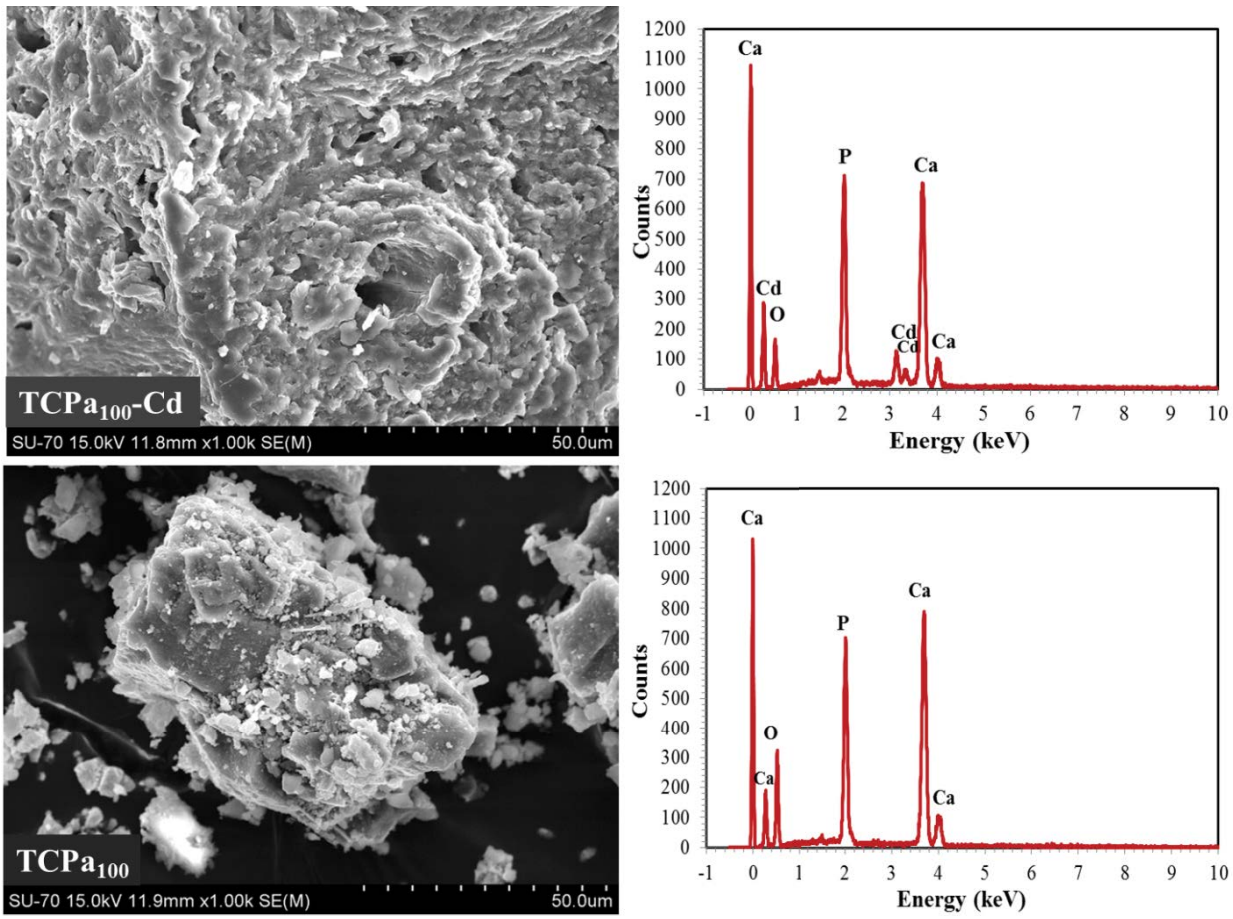

Fig. 10. Scanning electron micrographs (on the left side) and the corresponding energy-dispersive X-ray spectra (on the right side) of the adsorbent before ($TCPa_{100}$) and after interaction with cadmium ($TCPa_{100}$-Cd).

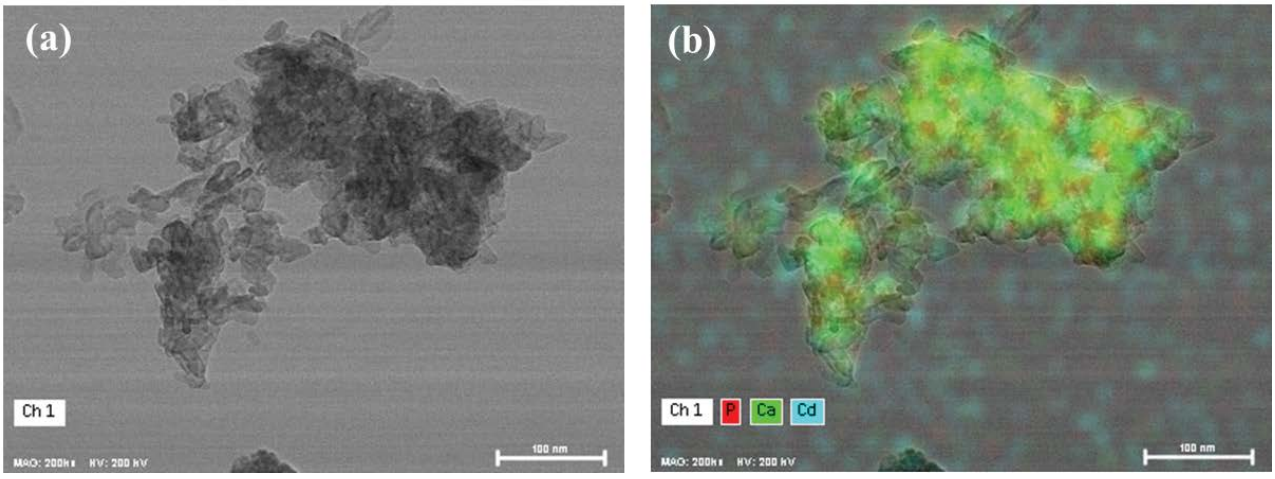

Fig. 11. (a) Transmission electron microscopy image of the $TCPa_{100}$-Cd sample after the adsorption process and (b) corresponding X-ray elemental mapping.

pH 4 to prevent excessive partial dissolution of the adsorbent in acid medium. The upper pH limit was selected to avoid the precipitation of Pb- and Cu-hydroxide forms, starting at slight alkaline medium (pH ~7.6). Hence, the affinity of the studied metal cations for $TCPa_{100}$ sample at pH 7 followed the sequence of Pb^{2+} (99.9%) > Cu^{2+} (99.2%) > Zn^{2+} (93%) > Cd^{2+} (90.1%), confirming that Pb^{2+} had the highest affinity to the adsorbent surface. Comparing the data obtained for lead, copper, zinc and cadmium, the removal percentages were strongly linked to their

Table 4
Physical characteristics of the studied metals

Cation	[a]RBS	[b]PE	[c]IR	[d]HR	[e]–logKH_2O,*M*
Ca^{2+}	1.44	1.00	0.99	4.12	12.7
Cd^{2+}	2.15	1.69	0.97	4.26	10.1
Cu^{2+}	2.66	1.90	0.73	4.19	7.5
Pb^{2+}	2.68	2.33	1.19	4.01	7.6
Zn^{2+}	2.20	1.65	0.74	4.30	9.0

[a]RBS: relative binding strength; [b]PE: Pauling electronegativity; [c]IR: ionic radius (Å); [d]HR: hydrated radius (Å); [e]–logKH_2O; *M*: log of the first hydrolysis constant.

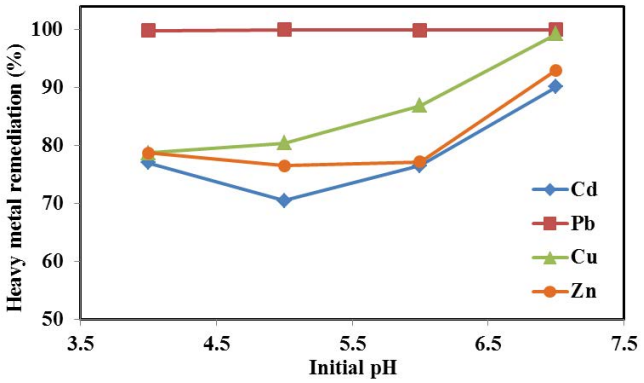

Fig. 12. Sorption of cadmium (Cd^{2+}), lead (Pb^{2+}), copper (Cu^{2+}) and zinc (Zn^{2+}) onto $TCPa_{100}$ under different pH values (Conditions: initial metal concentration = 100 mg L^{-1}; *V* = 100 mL; adsorbent dose = 0.2 g L^{-1}; contact time = 1 h).

electronegativity, their relative binding strength as well as their first hydrolysis constant [26].

3.5.2. Multi-component pollution systems

A synthetic wastewater containing 50 mg L^{-1} of Cd^{2+} and 25 mg L^{-1} of each Pb^{2+}, Zn^{2+} and Cu^{2+}, totalizing an overall concentration $[M^{2+}]_0$ of 125 mg L^{-1} was prepared and its initial pH value was adjusted to 7.00. Such synthetic wastewater reacted with $TCPa_{100}$ under the same testing conditions reported in Fig. 12 (*V* = 100 mL; adsorbent dose = 0.2 g L^{-1}; contact time = 1 h). The results displayed in Fig. 13 reveal that near total depollution has occurred for Pb^{2+} and Cu^{2+} ions in this multi-component system, whereas lower removal rates were observed for the other coexisting metal ions, 66.4% (Cd^{2+}) and 51% (Zn^{2+}). The adsorption rate of Cd^{2+} ions decreased from 96.1% measured for the single system (Fig. 6), to 66.4% in the multi-component solution. The ranking of metal remediation is Pb^{2+} (99.9%) ≈ Cu^{2+} (98.6%) > Cd^{2+} (66.4%) > Zn^{2+} (51%). The sequence order is slightly changed for the mixed metal sorption compared to single systems, since cadmium was better adsorbed by $TCPa_{100}$ sample over zinc. This new order is mainly related to the hydrated radius (Table 4).

The exchange of Ca^{2+} by divalent cations in the mixed systems might be facilitated when the hydrated radius is

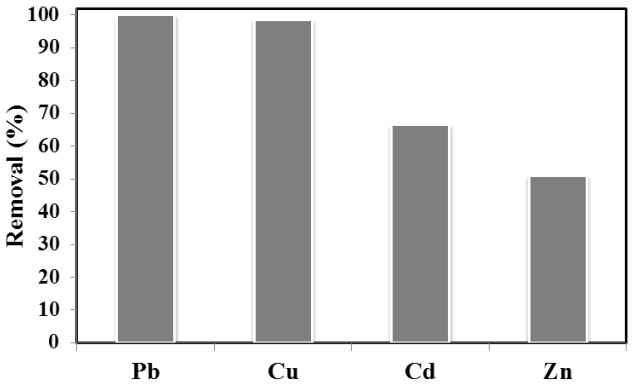

Fig. 13. Efficiency of the adsorption process in remediating a synthetic wastewater sample containing Cd^{2+}, Pb^{2+}, Cu^{2+} and Zn^{2+} under the following experimental conditions: $[M^{2+}]_0$ = 125 mg L^{-1}; *V* = 100 mL; adsorbent dose = 0.2 g L^{-1}; pH = 7; contact time = 1 h.

the smallest. Finally, under these testing conditions, the total depollution rate is about 76.4% and the calculated uptake capacity of heavy metals q_M^{2+} is 478 mg L^{-1}.

4. Conclusion

Calcination allows releasing the synthesis residues inserted into the structure of the Ca-apatites and is then likely to enhance their adsorption ability towards aqueous heavy metals. However, the rise of the calcination temperature induces concomitant decreases in the exposed surface area and total pore volume of the material, thus reducing the reactivity at the solid-liquid interface.

The results presented and discussed along this work enable to conclude that irrespective to the drastic decreases in the textural parameters, the Cd^{2+} uptake ability of TCPa powders from wastewaters is not much affected by the heat treatment temperature within the range from 100°C–900°C. Indeed, the prepared apatitic phase undergoes structural modifications upon calcination and, subsequently, the adsorption capacity might be more affected by the crystallographic tricalcium phosphate phase formed rather than by the undergone morphological changes. Since only a slight decrease in reactivity was observed, the consumption of energy during the calcination step can be prevented by using the apatitic sample dried at 100°C. Accordingly, the $TCPa_{100}$ powder was adopted for investigating the effects of other process parameters such as adsorbent dosage, initial metal concentration and temperature.

The equilibrium studies indicated that the Freundlich model fitted the experimental data better than Langmuir and DKR isotherms. The estimated value of the adsorption capacity at standard ambient temperature and pressure according to Langmuir model is 435 mg g^{-1}. Furthermore, the mean free energy value, *E*, provided by the DKR model is about 16 kJ mol^{-1}, suggesting a chemisorption reaction type. These results were strongly supported by the thermodynamic calculations, which revealed a chemical nature of the adsorption process involving strong attractive forces.

The adsorption ability of the selected material in up taking Pb^{2+}, Cu^{2+} and Zn^{2+} in single systems was also investigated. Except for Pb^{2+}, the removal capacity was found to be pH-dependent and the best results were observed at the upper pH limit (pH = 7) used in this work. Numerous studies reported that metal cations with ionic radii close to that of Ca^{2+} adsorb stronger. Accordingly, Cd^{2+} should adsorb more readily than Pb^{2+}, Cu^{2+} and Zn^{2+}, however, this is not confirmed in the present study. The experimental results showed that $TCPa_{100}$ sample's affinity followed the order $Pb^{2+} > Cu^{2+} > Zn^{2+} > Cd^{2+}$ which is consistent with electronegativity values and hydrolysis constants rather than the ionic radii. In multi-component pollution system, the coexisting metal ions had only a minor competitive effect on the adsorption of Cd^{2+} ions onto $TCPa_{100}$ and the ranking of metals removal was $Pb^{2+} > Cu^{2+} > Cd^{2+} > Zn^{2+}$. Indeed, Cd^{2+} and Zn^{2+} have similar hydrated radii of 4.26 and 4.30 Å, respectively, and lower electronegativities compared to Pb^{2+} and Cu^{2+}, which minimize their electron sharing and covalent bond formation with sorbent surface. Based on these results, $TCPa_{100}$ exhibited high removal efficiency in single and multi-pollution systems, and therefore, was found to be suitable for remediating heavy metals polluted waters.

References

[1] K.S. Egorova, V.P. Ananikov, Toxicity of metal compounds: knowledge and myths, Organometallics, 36 (2017) 4071–4090.

[2] M. Jaishankar, T. Tseten, N. Anbalagan, B.B. Mathew, K.N. Beeregowda, Toxicity, mechanism and health effects of some heavy metals, Interdiscip. Toxicol., 7 (2014) 60–72.

[3] N. Idrees, B. Tabassum, E.F. Abd-Allah, A. Hashem, R. Sarah, M. Hashim, Groundwater contamination with cadmium concentrations in some West U.P. Regions, India, Saudi J. Biol. Sci., 25 (2018) 1365–1368.

[4] S. Rajeshkumar, X. Li, Bioaccumulation of heavy metals in fish species from the Meiliang Bay, Taihu Lake, China, Toxicol. Rep., 5 (2018) 288–295.

[5] J.D.D. García, E. Arceo, Renal damage associated with heavy metals: review work, Rev. Colomb. Nefrol., 5 (2018) 43–53.

[6] C. Jalili, M. Kazemi, E. Taheri, H. Mohammadi, B. Boozari, A. Hadi, S. Moradi, Exposure to heavy metals and the risk of osteopenia or osteoporosis: a systematic review and meta-analysis, Osteoporos Int., 31 (2020) 1671–1682.

[7] M. Caffo, G. Caruso, G. La Fata, V. Barresi, M. Visalli, M. Venza, I. Venza, Heavy metals and epigenetic alterations in brain tumors, Curr. Genomics, 15 (2015) 457–463.

[8] S. Jebri, M. Jaouadi, I. Khattech, Precipitation of cadmium in water by the addition of phosphate solutions prepared from digested samples of waste animal bones, Desal. Water Treat., 217 (2021) 253–261.

[9] F. Liu, G. Zhang, Q. Meng, H. Zhang, Performance of nanofiltration and reverse osmosis membranes in metal effluent treatment, Chin. J. Chem. Eng., 16 (2008) 441–445.

[10] T.M. Zewail, N.S. Yousef, Kinetic study of heavy metal ions removal by ion exchange in batch conical air spouted bed, Alexandria Eng. J., 54 (2015) 83–90.

[11] R. Sánchez-Hernánde, I. Padilla, S. López-Andrés, A. López-Delgado, Single and competitive adsorptive removal of lead, cadmium, and mercury using zeolite adsorbent prepared from industrial aluminum waste, Desal. Water Treat., 126 (2018) 181–195.

[12] A. Bechrifa, M. Jemal, Enthalpy of formation and mixing of calcium-cadmium phosphoapatites, Phosphorus Res. Bull., 15 (2004) 113–118.

[13] S. Jebri, H. Boughzala, A. Bechrifa, M. Jemal, Structural analysis and thermochemistry of "A" type phosphostrontium carbonate hydroxyapatites, J. Therm. Anal. Calorim., 107 (2012) 963–972.

[14] S. Jebri, A. Bechrifa, M. Jemal, Standard enthalpies of formation of "A" type carbonate phosphobaryum hydroxyapatites, J. Therm. Anal. Calorim., 109 (2012) 1059–1067.

[15] Y. Zhu, B. Huang, Z. Zhu, H. Liu, Y. Huang, X. Zhao, M. Liang, Characterization, dissolution and solubility of the hydroxypyromorphite–hydroxyapatite solid solution $[(Pb_xCa_{1-x})_5(PO_4)_3OH]$ at 25°C and pH 2–9, Geochem. Trans., 17 (2016) 2–18.

[16] V. Stanić, S. Dimitrijević, J. Antić-Stanković, M. Mitrić, B. Jokić, I.B. Plećaš, S. Raičević, Synthesis, characterization and antimicrobial activity of copper and zinc-doped hydroxyapatite nanopowders, Appl. Surf. Sci., 256 (2010) 6083–6089.

[17] R. Aouay, S. Jebri, A. Rebelo, J.M.F. Ferreira, I. Khattech, Enhanced cadmium removal from water by hydroxyapatite subjected to different thermal treatments, J. Water Supply Res. Technol. AQUA, 69 (2020) 678–692.

[18] S.C. Liou, S.Y. Chen, Transformation mechanism of different chemically precipitated apatitic precursors into β-tricalcium phosphate upon calcination, Biomaterials, 23 (2002) 4541–4547.

[19] A.I. Adeogun, E.A. Ofudje, M.A. Idowu, S.O. Kareem, S. Vahidhabanu, B.R. Babu, Biowaste-derived hydroxyapatite for effective removal of Reactive Yellow 4 dye: equilibrium, kinetic, and thermodynamic studies, ACS Omega, 3 (2018) 1991–2000.

[20] D. Varrica, E. Tamburo, M. Vultaggio, I. Di Carlo, ATR–FTIR spectral analysis and soluble components of PM_{10} and $PM_{2.5}$ particulate matter over the urban area of Palermo (Italy) during normal days and Saharan events, Int. J. Environ. Res. Public Health, 16 (2019) 2507, doi: 10.3390/ijerph16142507.

[21] L. Jelinek, E. Kováts, True surface areas from nitrogen adsorption experiments, Langmuir, 10 (1994) 4225–4231.

[22] M. Dogan, M. Alkan, Adsorption kinetics of methyl violet onto perlite, Chemosphere, 50 (2003) 517–528.

[23] I. Mobasherpour, E. Salahi, M. Pazouki, Removal of divalent cadmium cations by means of synthetic nano crystallite hydroxyapatite, Desalination, 266 (2011) 142–148.

[24] T.B. Kinraide, U. Yermiyahu, A scale of metal ion binding strengths correlating with ionic charge, Pauling electronegativity, toxicity, and other physiological effects, J. Inorg. Biochem., 101 (2007) 1201–1213.

[25] H. El Boujaady, M. Mourabet, M. Bennani-Ziatni, A. Taitai, Adsorption/desorption of Direct Yellow 28 on apatitic phosphate: mechanism, kinetic and thermodynamic studies, J. Assoc. Arab Univ. Basic Appl. Sci., 16 (2014) 64–73.

[26] C. Appel, L.Q. Ma, R.D. Rhue, W. Reve, Sequential sorption of lead and cadmium in three tropical soils, Environ. Pollut., 155 (2008) 132–140.